ISRM International Symposium 2008
5th Asian Rock Mechanics Symposium (ARMS5), 24-26 November 2008 Tehran, Iran

INTERPRETATION OF MECHANICAL INTEGRITY TESTS

M.KARIMI-JAFARI[1], P.BEREST[2] B.BROUARD[3] and L.VAN SAMBEEK[4]

[1] *SOFREGAZ*
(Mehdi.KARIMI-JAFARI@sofregaz.fr)

[2] *LMS, Ecole Polytechnique, France*

[3] *BrouardConsulting*

[4] *RESPEC*

Abstract

Solution-mined caverns used for storing liquid hydrocarbons must be tested for tightness. The simplest test consists of rapidly increasing cavern pressure and monitoring further pressure evolution. A large leak results in a fast pressure drop rate. However, together with an actual leak, pre-existing and test-triggered phenomena contribute to cavern pressure evolution, making the apparent leak faster or slower than the actual leak. These phenomena can be accurately described and numerically computed.

Keywords: Salt caverns; Tightness tests; Salt creep.

1. Introduction

Solution-mined caverns are used world-wide to store liquid hydrocarbons. These caverns are tested on a regular basis to prove the absence of significant leaks. Various tightness tests are currently used Fig.1). The Nitrogen Leak Test consists of lowering a nitrogen column below the casing shoe in the annular space and tracking the nitrogen-brine interface. In this paper, the simplest tightness test (Liquid-Liquid Test) is discussed: the annular space is filled with a light hydrocarbon and, at the beginning of the test, cavern pressure rapidly is built up by p^1, and further pressure evolution as a function of time or $p = p(t)$ is recorded during several days [1]. A significant pressure drop rate is a clear sign of poor tightness. In fact, together with an actual liquid leak, several phenomena may explain the pressure drop observed after a cavern has been rapidly pressurized. The objective of this paper is to identify those phenomena that might contribute to the "apparent" leak and, when properly accounted for, can reduce the gap between the apparent (as-observed) leak and the actual leak.

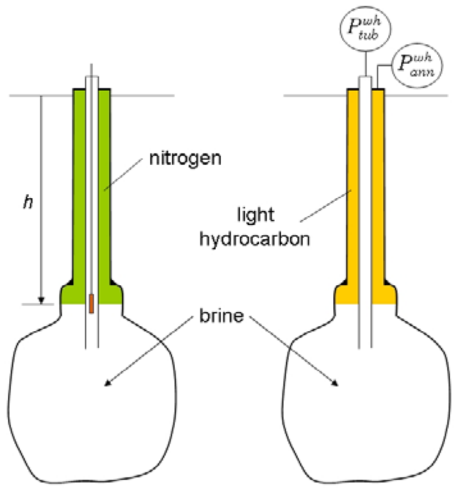

Figure 1. Nitrogen Leak Test and Liquid-Liquid Test

2. Pre-existing and test-triggered phenomena

A first group of phenomena pre-exist the test: they include brine thermal expansion (caverns are created by circulating cold soft water in a deep salt formation where geothermal temperature is warm.) and pre-existing salt creep.

A second group consists of test-triggered phenomena. They include transient brine permeation through the salt formation (pure rock salt permeability is exceedingly small; however salt-beds often contain a fair amount of insoluble rocks whose permeability is larger), additional dissolution (the amount of salt that can be dissolved in a given mass of water is a function of brine pressure; pressure build up in a closed cavern leads to additional dissolution; in the process the volume of cavern brine + dissolved salt decreases and pressure drops), brine cooling (a rapid pressure increase leads to an instantaneous adiabatic warming of cavern brine) and transient salt creep. According to the Le Chatelier-Braun principle, test-triggered phenomena make the apparent leak *smaller* than the actual leak.

3. Description of the various phenomena

3.1. *Cavern compressibility*

When a certain volume of brine or v^{inj} is injected in a closed cavern, cavern brine pressure increases by:

$$p = v^{inj} / \beta V_c \tag{1}$$

where V_c is the cavern volume and β is the factor of compressibility. In fact $\beta = \beta_c + \beta_b$ is the sum of brine compressibility factor plus cavern compressibility factor, which depends on cavern shape and rock mass elastic properties; $\beta_c = 1.3 \cdot 10^{-4}$/MPa , $\beta_b = 2.7 \cdot 10^{-4}$/MPa and $\beta = 4 \cdot \leq 10^{-4}$/MPa are typical.

3.2. *Brine thermal expansion*

The liquids (brine or hydrocarbons) contained in a salt cavern generally are colder than the rock mass [2]. In an idle cavern, cavern liquids gently warm to reach equilibrium with the surrounding rock mass. This process generally is slow. Heat transfer through the rock mass can be described by the conduction equation:

$$\partial T / \partial t = k_{salt}^{th} \Delta T \tag{2}$$

$k_{salt}^{th} = 3 \cdot 10^{-6}$ m^2/s is salt thermal diffusivity. In the cavern, brine temperature or T_b is homogeneous as brine effectively is stirred by thermal convection. The amount of heat transferred from the rock mass to the cavern can write:

$$\int_{\partial\Omega} K_{salt}^{th} \partial T / \partial n da = \rho_b C_b V_c \dot{T}_b \tag{3}$$

where $\rho_b C_b = 4.6 \times 10^6 \, J / °C / m^3$ is the volumetric heat capacity of brine and $K_{salt}^{th} = \rho_{salt} C_{salt} k_{salt}^{th}$ is the salt thermal conductivity; $\rho_{salt} C_{salt} = 2 \times 10^6 \, J / °C / m^3$ is the volumetric heat capacity of rock salt, making $K_{salt}^{th} = 3$ W/m/°C . When initial and boundary conditions are given, brine temperature evolution can be numerically computed. However orders of magnitude can easily be inferred from dimensional analysis. Let R be a characteristic dimension of the cavern (say, its radius). The warming process is governed by two characteristic times, $t_c = R^2 / \pi k_{salt}^{th}$ and $t_c^* = t_c / \chi$ where $\chi = \rho_{salt} C_{salt} / \rho_b C_b \approx 0.42$. These two characteristic times are not very different. Let T_R and T_b^0 be the average rock temperature at cavern depth and the initial brine temperature, respectively. During an initial t_c-long period of time, the brine warming rate typically is $\dot{T}_b \approx (T_R - T_b^0)/t_c$. Brine warming generates brine thermal expansion and brine pressure increase rate in a closed cavern approximately is:

$$\dot{p} = \alpha_b (T_R - T_b^0) / \beta t_c \tag{4}$$

where $\alpha_b = 4.4 \times 10^{-4} / °C$ is brine thermal expansion coefficient. Consider for instance an idealized spherical cavern, R = 20 m, V_c = 32,000 m^3, t$_c$ = 1 yr and $\dot{p} = 0.06$ Mpa/day , a pressure increase rate which can hide a significant leak (for instance, a $Q_{leak} = 36$ m^3 / yr *actual* leak generates a $\dot{p} = - Q_{act} / \beta V_c = - 0.008$ MPa/day pressure drop rate).

3.3. *Additional dissolution*

Together with transient creep, additional dissolution is the most significant "test-triggered" phenomenon. The amount of salt that can be dissolved in a given mass of water is an increasing function of brine pressure (and temperature): pressure build up in a closed cavern filled with saturated brine leads to additional dissolution; in the process, the volume of cavern brine + dissolved salt decreases, more room is provided to the cavern brine, and, after some time, brine pressure drops. A new equilibrium is reached after several days. Magnitude of the pressure drop is easy to quantify; assessing additional dissolution kinetics is more difficult. Consider a cavern filled with saturated brine. A volume of brine, or v^{inj}, is injected rapidly in the cavern whose pressure instantaneously builds up by $p^1 = v_{inj} / \beta V_c$. After several days, cavern brine is saturated again and cavern final pressure is p^f. In the process, brine concentration, or c_{sat} and brine density, or ρ_{sat} increase by: $c_{sat}^f - c_{sat}^0 = c_{sat}^0 \psi p^f$ and $\rho_{sat}^f - \rho_{sat}^0 = \rho_{sat}^0 a_s p^f$, respectively. Mass conservation leads to [2]:

$$p^f = v_{inj} / (\beta_c + a_s - \varpi) V_c^0 \quad (5)$$

$$\bar{\varpi} = (1 - \rho_{sat}^0 / \rho_{salt}) c_{sat}^0 \psi (1 - c_{sat}^0) \quad (6)$$

salt density is $\rho_{salt} = 2200 kg / m^3$, $c_{sat}^o = 0.2655,\ \rho_{sat}^0 = 1,200 \text{ kg/m}^3$, $\psi = 2.6 \cdot 10^{-4} \text{/MPa}$, $a_s = 3.16 \cdot 10^{-4} \text{/MPa}$. The apparent leak caused by additional dissolution is: $v_{leak}^{app} = 0.043 v_{inj}$. For instance, when a $v^{inj} = 100 \text{ m}^3$ volume of brine is injected in a $V_c^o = 50,000 \text{ m}^3$ cavern, the initial pressure build-up is $p^1 = 5 \text{ MPa}$, the apparent leak is $v_{leak}^{app} = 4.3 \text{ m}^3$ and the final pressure increase is p^f = 4.95 MPa. From the point of view of tightness test interpretation, a key question is: how long does the saturation process lasts. The answer is difficult. Brine saturation occurs through multiple processes, including diffusion inside the boundary layer at the cavern wall and convection and diffusion through the cavern. The whole process is difficult to compute exactly; its duration is likely to depend on cavern size and age. Based on a few field data we propose to characterize the dissolution process using the following differential equations:

$$\partial c / \partial t = (c_{sat} - c) / t^{diss} \quad (7)$$

$$\partial \rho / \partial t = \rho_{sat}^0 \beta_b \partial p / \partial t + (\rho_{sat}^f - \rho) / t^{diss} \quad (8)$$

where t_c^{diss} is a constant of empirical origin, t_c^{diss} = 2.5 days typically.

3.4. . *Adiabatic compression*

When pressure rapidly is increased in a fluid-filled cavern by p, cavern brine experiences an instantaneous temperature increase. This temperature increase, or θ, results from the first law of thermodynamics:

$$\rho_b C_b \theta = \alpha_b T_b p \quad (9)$$

When the cavern is filled with brine, this temperature increase is a fraction of a degree Celsius, or $\theta / p = 3 \times 10^{-2}$ °C/MPa. Even though small, this temperature may be significant because it is achieved during a short period of time: it is followed by brine cooling and a subsequent pressure drop in a closed cavern. This transient pressure drop is quite fast during a couple of days and may lead to misinterpretation of a tightness test. Brine cooling is independent from the pre-existing brine warming, as the equations which describe conduction are linear. In the case of an idealized spherical cavern, in the first days following pressure build-up, pressure decrease rate due to brine cooling can write: $\dot{p}_i(t) = -3 \chi \alpha_b^2 T_b p^1 \sqrt{1 / t t_c^{th}} / \pi \beta \rho_b C_b$. In fact this rate is slow, except during the first hours following the initial pressure build-up.

3.5. *Brine permeation through the cavern walls*

In the context of a tightness test, it is believed that leaks occur mainly through the cemented casing; however, leaks through the formation itself must be assessed. Pure rock salt exhibits a very low permeability. Permeability magnitudes as small as $K_{salt}^{hyd} = 10^{-22}$ to 10^{-20} m^2 are reported. Steady-state leaks (i.e., when the cavern remains idle during a long period of time) are extremely small. However transient leaks following a rapid pressure build-up may be significant. To allow simple estimations, we assume the following: Darcy's law for fluid flow through porous media holds:

$$\partial p / \partial t = k_{salt}^{hyd} \Delta p \qquad (10)$$

where $k_{salt}^{hyd} = MK_{salt}^{hyd} / \mu_b$ is the hydraulic diffusivity; $\mu_b \approx 1.4 \times 10^{-3}$ Pa.s is brine viscosity and M is rock salt Biot's modulus; before the test began, pore pressure equals cavern pressure; brine outflow from the cavern is:

$$Q_{perm} = \int_{\partial\Omega} K_{salt}^{hyd} \partial p / \partial n \, da \qquad (11)$$

The system of equations to be solved is very similar to the system which governs brine temperature evolution; however, in sharp contrast with the thermal phenomena, the constants such as k_{salt}^{hyd}, K_{salt}^{hyd} or M are poorly known, making any quantitative assessment difficult. Here again the pressure decrease rate is small, except during the first hours following pressure build-up.

4. Creep

At this step, a few comments on the mechanical behaviour of salt are helpful. No other rock has given rise to such a comprehensive set of lab experiments, motivated, to a large extent, by the specific needs of nuclear waste storage.

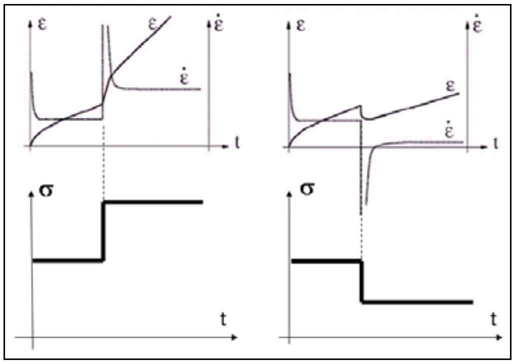

Figure 2 - Strain and strain rate during a creep test.

Most experts agree on the main features of steady-state rock-salt behaviour:

- In the long term, rock-salt flows even under very small deviatoric stresses (rock-salt behaves as a viscous liquid).
- Creep rate is a highly non-linear function of applied deviatoric stress and temperature (rock-salt is a non-newtonian liquid).
- Steady-state creep is reached after several weeks or months when a constant load is applied to a sample; it is characterized by a constant creep rate.
- Transient creep is triggered by any rapid change in the applied stress. Transient creep is characterized by high initial rates (following a load increase) or by "reverse" initial rates (following a load decrease; "reverse creep" refers to a transient sample height increase following a decrease in the applied stress during an uniaxial test performed on a cylindrical sample, even though the applied stress is compressive) that slowly decrease or increase to reach steady-state creep (Fig.2).

4.1. *Steady-state creep*

Main features of steady-state creep are captured by the following simple model (Norton-Hoff power law):

$$\dot{\varepsilon}_{ss}^{ij} = 3A\exp\left(-Q/RT\right)\left(\sqrt{3J_2}\right)^{n-1} s_{ij}/2 \qquad (12)$$

Where J_2 is the second invariant of the deviatoric stress tensor; *A, n, Q/R* are model parameters; *n* is in the range *n* = 3-6. Note that when a cavern (instead of a cylindrical sample) is considered, "transient" behaviour can be observed following a cavity pressure change – although Norton-Hoff constitutive behaviour includes no transient rheological behaviour. The reason is that after a pressure change, stresses redistribute slowly inside the rock mass. Such a transient behaviour is called "geometrical".

4.2. *Munson transient model*

The Norton-Hoff model does not account for rheological transient creep. Better accounting for in situ observations requires that transient creep be incorporated in the constitutive model. Munson and Dawson [4] suggested the following model:

$$\dot{\varepsilon}_{vp}^{ij} = F\dot{\varepsilon}_{ss}^{ij}$$

$$F = e^{\Delta(1-\varsigma/\varepsilon_t^*)^2} \quad \text{when } \varsigma \le \varepsilon_t^*$$
$$F = e^{-\delta(1-\varsigma/\varepsilon_t^*)^2} \quad \text{when } \varsigma \ge \varepsilon_t^* \qquad (13)$$

$$\dot{\varsigma} = (F-1)\dot{\varepsilon}_{ss}, \quad \dot{\varepsilon}_{ss} = A\exp\left(-Q/RT\right)\left(\sqrt{3J_2}\right)^n$$
$$\varepsilon_t^* = K_0 e^{cT}\sigma^m, \ \Delta = \alpha_w + \beta_w Log_{10}\sigma/\mu, \ \delta=\delta_0$$

Note that this model accounts for "transient" creep, but predicts no "reverse creep" following a stress decrease.

4.3. *A modified version of the Munson model*

Munson *et al.* [6] suggested a modified model taking into account the onset of "reverse creep" following a stress drop (i.e., a rapid pressure build up in a closed cavern). We propose a slightly modified version of this law that allows for simple computations:

$$F = 1-(1-\varsigma/\varepsilon_t^*)^p/(1-k)^p \ \text{ when } \varsigma > \varepsilon_t^* \qquad (14)$$

and reverse creep appears when $\varsigma > k$. This "transient" model includes several new constants: a first group of constants, or $K_0, c, m, \alpha_w, \beta_w$ were inferred by Munson from lab tests performed on Gulf Coast salt. A second group of constants, or *k,p* can be back-calculated from the results of in-situ tests.

5. Examples

Pressure evolutions following the pressure build-up performed at the beginning of a tightness test were computed. The phenomena described above (brine warming, brine cooling following adiabatic compression, brine permeation, transient creep, additional dissolution) were taken into account. Two examples are described below. In all these examples, the actual liquid leak rate is assumed to be 164 m^3/year (1000 bbls/year; this figure often is considered as the "Maximum Allowable Leak Rate", [1]). On each figure, in the right hand side rectangle, the effects contributing to pressure drop rate during a tightness test are listed; in most cases they include, together with the actual pressure drop rate (164 m^3/year) which appears in the lowest part of the rectangle, such effects as transient "reverse" creep, additional dissolution, transient permeation and brine cooling following adiabatic compression; rather than the contribution of each phenomenon to the pressure evolution, or "$\dot{P} < 0$", the equivalent flow rates or "$Q = \beta V_c \dot{P}$" are indicated. On the left hand side, in the upper part of the rectangle, phenomena contributing to pressure build-up rate, or "$\dot{P} > 0$" are listed; in most cases they include pre-existing creep and brine warming. The difference between factors contributing to pressure drop and factors contributing to pressure build up is the "apparent leak" which appears in the lower part of the left hand side rectangle. Comparison between the apparent leak and the actual leak is of special interest in the context of tightness test interpretation.

5.1. *Example 1*

This cavern is 600-m deep and its volume is 14,137 m^3 (100,000 bbls). It was leached out in 150 days. One month after the cavern was washed out, a tightness test is performed: cavern pressure is built up through brine injection from 7.2 MPa (pre-test pressure) to 10.2 MPa (testing pressure); brine injection lasts 2 hours. Three days after the pressure was built up, the effects of the transient phenomena triggered by the test are responsible for a 4 + 33 + 3 + 11 = 51 m^3/year apparent leak rate (their contribution was 325 m^3/year on Day 1). Brine warming still is effective, as the test is performed a few weeks after leaching was completed. The as-measured leak rate (42 m^3/year) underestimates the actual leak rate (164 m^3/year): in this small and young cavern, the effects of brine warming are able to hide a large part of the actual leak (Figure 3).

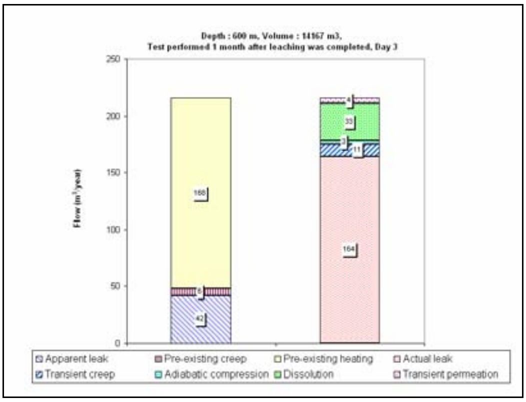

Figure 3 – Example 1.

5.2. *Example 2*

Cavern depth is 1200 m and its volume is 525,583 m^3; the cavern was washed out in 700 days. The test is performed 5 years later. Before the test, a pre-pressurization period was managed: cavern pressure, which was 14.4 MPa before the test, was first pre-pressurized to 95% of the final testing pressure and pressure was kept constant during 15 days to mitigate the effects of transient phenomena; at the end of this period, cavern pressure was built up to its final figure (20.4 MPa) in two hours. In this very large cavern, brine warming still is effective even 5 years after leaching was completed. Test-triggered effects are more or less proportional to cavern volume: although a pre-pressurization period is observed, these effects are still much larger than the effects of the actual leak, as the actual leak is assumed in these examples to be independent from cavern size. In a very large cavern, this testing procedure (pressure decrease observation) cannot be recommended as the apparent leak may be very different from the actual leak. Even a long testing period (several weeks) is not able to significantly improve test accuracy (Figure 4).

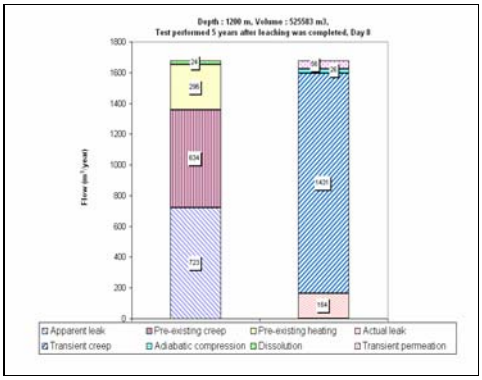

Figure 4 - Example 2.

6. Conclusion

It was proved that transient phenomena – other than the actual leak – can strongly influence cavern pressure evolution after a rapid pressure build up. Additional dissolution and "reverse" creep make the apparent leak faster than the actual leak; their role is especially significant in a large and deep cavern. Pre-existing brine warming makes the apparent leak slower than the actual leak; its role is pre-eminent in a small and freshly washed-out cavern. These phenomena can be accounted for, allowing for a better assessment of cavern tightness.

Acknowledgements

This work was supported by the Solution Mining Research Institute.

Appendix: an *in situ* test

An *in situ* test illustrates the various factors described above. The EZ53 cavern was leached out in 1982; it belongs to the Etrez site operated by Gaz de France. It is a small cavern (7,500 +/500 m^3) and its average depth is H = 950-m. At this depth, rock temperature is T_R = 45°C. Cavern was kept idle after the leaching phase was completed. Cavern brine slowly warms up; temperature was recorded from time to time. It was 35.22°C on September 8, 1982 (day 94 after leaching ended) and 36.09°C on day 123. The average temperature increase rate during this period was $\dot{T}_b = 0.032$°C/day, a figure consistent with back-of-the-envelope calculations, and a $Q_{th} = \alpha_b V_c \dot{T}_b$ = 100 litres/day brine outflow rate could be expected. In fact the actual rate was a little faster (Fig.5); the difference was due to cavern creep closure. The annular space was filled with a light hydrocarbon (whose density was ρ_h = 850 kg/m^3) whose pressure at the well-head was approximately $p = g\,H\,(\rho_b - \rho_h)$ = 3.4 MPa; the brine-filled central tube well-head was opened to atmosphere and brine was allowed to outflow from the cavern. On day 93, a valve was opened to partially remove the hydrocarbon; the hydrocarbon pressure at the well head suddenly dropped to atmospheric pressure; the air/brine interface in the central string dropped by $h = p / g(\rho_b - \rho_h)$ = 290 m to balance the pressure drop in the annular space.

The hydrocarbon outflow rate was measured from day 93 to day 254 (Fig. 5). During a dozen of days, the hydrocarbon flow-rate is very fast, a clear sign of large transient effects in the cavern. The flow-rate more or less stabilizes after this initial period. It is larger than what the brine flow was before the pressure drop, a clear proof of the non-linear effect of cavern pressure on cavern creep closure rate (at a 950-m depth, the geostatic pressure is $P\infty$ = 21 MPa. Cavern pressure was P = 11.4 MPa before the pressure drop and P = 11.4 – 3.4 = 8 MPa after the pressure drop). The initial cavern pressure, or P = 11.4 MPa, was restored on day 253. This phase of the test is of special interest as it simulates the effect of a rapid cavern pressure increase. The annular space was closed at the wellhead and the central tubing was filled with brine. After this injection was completed, the brine level dropped in the central tubing (an effect of additional dissolution and transient cavern creep). Every 24 hours, brine was added to fill the central tubing. The daily amount of brine to be added gradually decreased, as transient effects slowly vanish. Eventually, 10 days after the first filling took place (day 263), brine was again expelled from the well-head and a constant brine-flow rate was observed, equivalent to 52 litres per day instead of 100-litres per day observed before the test: thermal expansion is less and less active.

We focus on transient phenomena, which are especially effective during the day 253 to 264 period. The daily amount of brine injected (+) or withdrawn (-) during this period was carefully measured: -393-222-171-138-32-32-33-33-34-68+31+48 = -1077 litres. During the same 12-day period, the brine flow rate due to brine warming should have been 52 litres/day (as it will be a few days later), or 624 litres during the 12-day period. As a whole, the cavern volume increase is 1077 + 624 = 1700 litres. A part of this volume increase is due to additional dissolution. At the beginning of this phase, brine was rapidly poured into the central tubing, resulting in an increase in cavern pressure by p = 3.4 MPa. The injection was rapid: no additional dissolution had time to take place during the rapid injection. In the following days, brine was injected in the cavern to keep cavern pressure constant. The volume of brine to be injected to balance the effect of additional dissolution is $v^{inj} - v_0^{inj} = (a_s - \varpi) V_c^0 p$, or 444 litre: transient creep is responsible for a cavern volume increase by 1700 – 444 = 1350 litres which is spread over a 10-day long period of time. After this period, cavern volume decreases again. Numerical computations were performed.

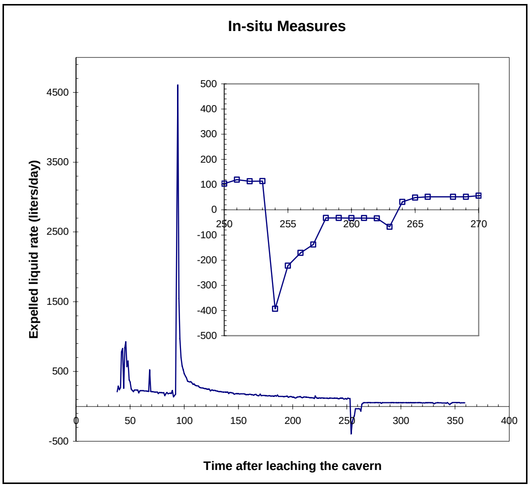

Figure 5. Liquid outflow rate (as-measured)

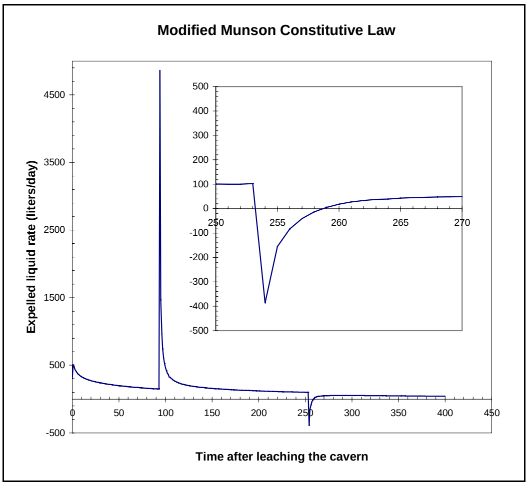

Figure 6 - Liquid outflow rate (computed)

Cavern creation is simulated by a 3-month long decrease in cavern pressure from the geostatic figure ($P_\infty = 22\ \text{MPa}$) to P = 11.4 MPa. Rock temperature and brine temperature at the end of the leaching phase are $T_b^0 = 26.5°\text{C}$ and $T_R = 45°\text{C}$, respectively. Pressure history is as during the actual test. Brine warming and additional dissolution are taken into account. The parameters of the Norton-Hoff law are E = 25,000 MPa, ν = 0.25, A = 0.64 /MPa$^{3.1}$/yr, n = 3.1, Q/R = 4100 K; these figures were obtained from laboratory tests performed on Etrez salt samples. The Munson model parameters are: m = 3.5, K_o = 6.7 10^{-11} /MPa$^{3.5}$, C = 0.0315, α_w = 10, β_w = 0, δ = 0.58. The modified model parameters are p = 5 and k = 4. These figures result from a (single) creep test performed on an Etrez salt sample; back-calculations also were used. A good fit with in situ data can be reached (Fig. 6).

References

1. Thiel W.R., 1993. Precision Methods for Testing the Integrity of Solution Mined Underground Storage Caverns. *7th Symposium. on Salt, Elsevier, Kyoto, Vol. I,* 377-383.

2. Van Sambeek L., P. Bérest and B. Brouard, 2005. Improvements in mechanical integrity tests for solution-mined caverns. *SMRI Topical Report RSI-1799, 152 pages.*

3. Munson D.E. and P.R. Dawson, 1984. Salt Constitutive Modeling using Mechanism Maps. *Proceedings 1st Conference on the Mechanical Behaviour of Salt, Trans Tech. Pub.*, 717-737.

4. Munson D.E., K.L. De Vries, A.F. Fossum and G.D. Callahan, 1996. Extension of the Munson-Dawson model for treating stress drops in salt. *Proceedings 3rd Conference on the Mechanical Behaviour of Salt, Trans Tech. Pub.*, 31-44.

5. Hugout B., 1988. Mechanical behavior of salt cavities -in situ tests- model for calculating the cavity volume evolution. *Proceedings 2nd Conference on the Mechanical Behaviour of Salt, Trans Tech. Pub*. 291–310.